The Mechanisms of Colorectal Cancer Cell mesenchymal-epithelial Transition Induced by Hepatocyte Exosome-derived miR-203a-3p

Heyang Xu
Sun Yat-sen University
Qiusheng Lan
Sun Yat-sen University
Yongliang Huang
Southern Medical University
Yang Zhang
Guangzhou Blood Center
Yujie Zeng
Sun Yat-sen University
Pengwei Su
Sun Yat-sen University
Ziqiang Chu
Sun Yat-sen University
Wei Lai
Sun Yat-sen University
Zhonghua Chu (sumschuzhonghua@hotmail.com)
Sun Yat-sen University

Research Article

Keywords: miR-203a-3p, exosome, mesenchymal-to-epithelial transition, colorectal cancer

Posted Date: February 9th, 2021

DOI: https://doi.org/10.21203/rs.3.rs-147649/v1

Version of Record: A version of this preprint was published at Journal of Bio-X Research on September 1st, 2018. See the published version at https://doi.org/10.1097/JBR.0000000000000013.

Abstract

Background: Liver metastasis is the most common cause of death in patients with colorectal cancer (CRC). Phosphatase of regenerating liver-3 induces CRC metastasis by epithelial-to-mesenchymal transition, which promotes CRC cell liver metastasis. Mesenchymal-to-epithelial transition (MET), the opposite of epithelial-to-mesenchymal transition, has been proposed as a mechanism for the establishment of metastatic neoplasms. However, the molecular mechanism of MET remains unclear.

Methods: Using Immunohistochemistry, western blotting、invasion assays, real-time quantitative PCR, chromatin immunoprecipitation, luciferase reporter assays, human miRNA arrays, and xenograft mouse model, we determined the role of hepatocyte exosome-derived miR-203a-3p in CRC MET.

Results: In our study, we found that miR-203a-3p derived from hepatocyte exosomes increased colorectal cancer cells E-cadherin expression, inhibited Src expression, and reduced activity. In this way miR-203a-3p induced the decreased invasion rate of CRC cells.

Coclusion: MiR-203a-3p derived from hepatocyte exosomes plays an important role of CRC cells to colonize in liver.

Introduction

Liver metastasis is the main cause of death in patients with colorectal cancer (CRC). Once patients are diagnosed with colorectal liver metastases, the 5-year survival rate is 11.7%[1,2] .Therefore, it is important to successfully identify the signaling pathway leading to CRC cell seeding in the liver; this information may pave the way to find effective therapies for patients with colorectal liver metastases. Studies have revealed that epithelial-to-mesenchymal transition (EMT) occurs in the process of CRC liver metastasis.[3] Further studies indicated that during the process of EMT, epithelial cells lose their epithelial traits and acquire mesenchymal characteristics to gain migratory and invasive properties.[4] At the same time, the morphology of tumor cells changes from epithelial-like to fibroblast-like, which may favor invasion and metastasis and allow the cells to establish secondary tumors at distant sites.[5] It has been demonstrated that cancer cells down-regulate E-cadherin, which is a hallmark of EMT and is associated with tumor cell invasion and metastasis.[6] However, once cancer cells colonize to specific organs, the re-expression of E-cadherin can be observed in the metastasis sites, indicating that cancer cells undergo the phenotypic mesenchymal-to-epithelial transition (MET), which is regulated by the tumor microenvironment.

Phosphatase of regenerating liver-3 (PRL-3) belongs to the protein tyrosine phosphatase family, which plays critical roles in the signal induction leading to the tyrosine phosphorylation of down-stream molecules.[7] PRL-3 has been shown to be overexpressed in the liver metastases of CRC but seldom expressed in the corresponding primary tumors or normal colorectal epithelium, indicating that it participated in the progression and metastasis of tumor cells.[8] Recently, considerable evidence has suggested that EMT is the mechanism by which PRL-3 promotes CRC metastasis. For example, PRL-3

regulated the phosphoinositide 3-kinase (PI3k)/AKT pathway to modulate E-cadherin expression.[9] More obviously, PRL-3 can regulate cadherin directly to enhance the invasion ability of CRC.[10] The expression of PRL-3 has been found to be positively correlated with tumorigenesis and metastasis in various tumors, including CRC, gastric cancer and ovarian cancer.[11-13] Our previous study also revealed that PRL-3 could activate the NF-κB pathway to induce KCNN4 expression, leading to the inhibition of E-cadherin expression and the promotion of CRC liver metastasis.[14] Although various signaling pathways have been implicated in PRL-3-induced EMT and it is well known that cancer cells need to undergo MET before colonizing the liver, whether PRL-3 regulates the progression of MET remains unknown. A recent study has revealed that PRL-3 could induce the activation of the epidermal growth factor receptor (EGF)/EGFR (epidermal growth factor receptor) signaling pathway; this finding indicates that PRL-3 may be involved in the progression of MET.[15]

EGFR is a receptor tyrosine kinase that can initiate pleiotropic intracellular signaling leading to defects associated with pathologies such as cancer.[16] Once EGFR signaling is activated, the downstream molecules, such as mitogen-activated protein kinases, PI3K-AKT, and Jak-Stat, are also activated.[17] The EGFR pathway has emerged as a key anticancer target for blocking the invasion and proliferation of tumor cells. Furthermore, it has been shown that effective targeted therapies against EGFR depend on the KRAS and BRAF status in patients with metastatic CRC and lung cancer, indicating that mutations could influence the activation of the EGFR pathway.[18] The EGF/EGFR signaling pathway was also found to induce EMT in several tumor types, including CRC, through the regulation of E-cadherin expression.[19] Interestingly, when cancer cells were co-cultured with hepatocytes, the activation of the EGFR signaling pathway was inhibited. At the same time, the expression of E-cadherin was induced, indicating that the EGF/EGFR pathway can regulate E-cadherin expression.[20] However, the specific mechanism is unclear.

Exosomes are small vesicles secreted by cell endosomes that range between 40 and 100 nm in diameter.[21] Studies have found that exosomes can regulate target cells directly through receptor combination or by transferring various bioactive molecules, such as proteins, mRNAs and circRNAs, into the target cells.[22] MicroRNAs (miRNAs) are non-coding single-stranded RNAs that are encoded by endogenous genes. miRNAs has been shown to play an important regulatory role in gene expression by binding to the 3'-UTRs (untranslated regions) of their target mRNAs.[23] It has been demonstrated for the first time that the dysregulation of miRNAs plays a very important role in the development of tumors.[24] Regarding tumor metastasis, miRNAs, such as miR-155, miRNA-200, and miR-205, can promote/inhibit the metastasis of malignant tumors by regulating EMT through RhoA or by regulating the expression of the E-cadherin transcription receptors ZEB1 and ZEB2.[25]

In this study, we aimed to explore the mechanisms of CRC cell MET, which facilitates cancer cell colonization to the liver.

Materials And Methods

Cells and cell culture/co-culture conditions

Stable cells (vector-transfected and PRL-3-expressing cells) were established using LoVo cells (Guangzhou Cellcook Biotech Co. Ltd) as described previously.[26] G418 cells were purchased from Sigma (St Louis, MO, USA). Cells were maintained in RPMI 1640 (HyClone, Logan, UT, USA) with 10% fetal bovine serum (FBS; Gibco, Carlsbad, CA, USA) at 37°C in a humidified incubator with 5% CO_2. The LO2 cell line (Guangzhou Cellcook Biotech Co. Ltd) was maintained in DMEM (HyClone, Logan, UT) containing 10% FBS. Co-culture analysis was performed in 6-well plates with transwell chambers (0.4-μm pore size, Corning, Canton, NY, USA). Cancer cells (1×10^5) were plated in the lower chamber of each well in 2000 μL of complete medium with 10% FBS and allowed to attach overnight. The next day, LO2 cells were plated at 5×10^4 cells per well in 1500 μL of complete medium in the upper chambers. The medium was replenished every 2 days. The PKC inhibitor GF109203X was obtained from Sigma. Recombinant human EGF protein was obtained from PeproTech (Rocky Hill, NJ, USA).

CRC samples

CRC samples were obtained from patients who were diagnosed with CRC and then underwent elective surgery at the Department of Gastroenteropancreatic Surgery, Sun Yat-sen Memorial Hospital, Sun Yat-sen University, between July 2006 and June 2010. The protocol was approved by the Ethics Committee of Sun Yat-Sen Memorial Hospital, China (Approve No.179). Seventy-five primary CRC samples (stage I, n = 12; stage II, n = 15; stage III, n = 25 and stage IV, n = 23) and 23 corresponding colorectal liver metastasis samples from stage IV patients were obtained from surgically resected specimens for immunohistochemistry.

Immunohistochemistry

Paraffin-embedded patient samples were obtained from Sun Yat-Sen Memorial Hospital. Colorectal tumor specimens were fixed in formalin and embedded in paraffin. After that, the tissue sections were deparaffinized in xylene for 10 min and then subjected to antigen retrieval by boiling in 0.01 M citric buffer (pH 6.0). Endogenous peroxidase activity in the samples was blocked with 3% hydrogen peroxide in PBS and 0.05% Tween 20 for 30 min. The samples were then washed with PBS and blocked for 30 min with 20% normal goat serum at room temperature, followed by incubation with primary antibodies against PRL-3, p50, p65 (Abcam, Cambridge, MA, USA), E-cad (Santa Cruz, California, CA, USA), p-EGFR and VEGF-A (Cell Signaling Technology, Cambridge, MA, USA) at a dilution of 1:100 in a humidified chamber overnight at 4°C. The next day, the sections were washed with PBS, incubated with peroxidase-conjugated secondary antibodies for 2 h at room temperature and then rinsed with PBS. Finally, the DAB Plus substrate staining system (Abcam, Cambridge, MA, USA) was used to stain the samples according to the manufacturer's instructions. All tissue sections were counterstained with hematoxylin and mounted with aqueous mounting media. The tissue sections were scored quantitatively according to the

percentage of positive cells and staining intensity. The intensity of staining was scored from 0-3 (I0, I1-3): 0 (no staining), 1 (weak staining = light yellow), 2 (moderate staining = yellow brown) and 3 (strong staining = brown). The proportion of the tumor stained at a particular intensity was recorded in 5% increments using a range of 0–100 (P0, P1–3). The final H score (range 0–300) was calculated for each intensity and proportion of the area stained (H score = I1×P1 + I2×P2 + I3×P3).

Western blot analysis

Cells were washed three times with cold PBS and lysed on ice with RIPA buffer containing 1% PMSF and a proteinase inhibitor cocktail. Sample protein concentrations were determined by Bradford assays.[26] Forty-microgram samples for each lane were boiled for 5 min in sample buffer. The denatured proteins were then separated by 10% or 12% sodium dodecyl sulfate-polyacrylamide gel electrophoresis and transferred onto polyvinylidene fluoride membranes. Nonspecific reactivity was blocked using 5% bovine serum albumin in a TBST buffer. The membranes were then incubated with the relevant primary antibodies overnight at 4°C. Following incubating with a horseradish peroxidase-conjugated secondary antibody at a 1:5000 dilution for 2 h at room temperature, the labeled proteins were visualized by chemiluminescence (American Bioscience, Piscataway, NJ, USA) western blotting detection reagents. Anti-GAPDH (mice, Abcam, Cambridge, MA, USA) was used to ensure equal amounts of protein were present for each sample. The protein amounts were estimated through densitometry as the ratio of the detected protein/GAPDH. Anti-vimentin, anti-EGFR, anti-Snail, anti-p-AKT, anti-AKT, anti- activated extracellular signal-regulated kinase (p-Erk1/2), anti-Erk1/2, anti-p-PKC, anti-PKC, anti-p-GSK-3β and anti-GSK-3β antibodies which were obtained from Abcam (mice, Cambridge, MA, USA). Incubations were substrate with ChemiDoc XRS+ imaging system (Bio-Rad Laboratories, Hercules, CA, USA) were used to detect immunoreactive bands.

Isolation of exosomes from medium and serum

Exosomes were isolated from cell culture medium by differential centrifugation. After removing cells and other debris by centrifugation at 300 × g and 3000 × g, the supernatant was centrifuged at 10,000 × g for 30 min to remove shedding vesicles and other larger-sized vesicles. Finally, the supernatant was centrifuged at 110,000 × g for 70 min (all steps were performed at 4°C); exosomes were collected from the pellet and re-suspended in PBS. Sr-exosomes were isolated by using an exosome isolation kit (Thermo, Waltham, MA, USA).

Luciferase assay

The reporter plasmid containing the predicted miR-203a-3p targeting regions was designed by Genescript (Nanjing, China). Part of the wild-type and mutated 3’-UTR of Src was cloned immediately downstream of the firefly luciferase reporter. A total of 2 mg of the β-galactosidase expression vector (Ambion) was used

as a transfection control. For the subsequent luciferase reporter assays, 2 mg of the firefly luciferase reporter plasmid, 2 mg of the β-galactosidase vector and equal doses (200 pmol) of the mimics, inhibitors or scrambled negative control RNA were transfected into the prepared cells. At 24 h after transfection, the cells were analyzed by using a dual luciferase assay kit (Promega) according to the manufacturer's instructions. Each sample was prepared in triplicate, and the entire experiment was repeated three times.

Invasion assays

Transwell chambers (BD Biosciences, Franklin Lakes, NJ, USA) were used to measure the ability of cells to invade in cell invasion assays. A total of 1×10^5 cells in 0.2 mL of serum-free RPMI 1640 medium were added to the upper chambers (with Matrigel [Collaborative Biomedical Products, Bedford, MA, USA]). The lower chambers contained 0.8 ml of medium with 10% FBS. After incubation at 37°C and 5% CO_2 for 24 h, the cells that invaded to the lower chamber were fixed in 4% paraformaldehyde and stained with 0.1% crystal violet in methanol. The cell counts are expressed as the mean number of cells per field of view. Three independent experiments were performed, and the data are presented as the mean standard deviation.

Immunofluorescence analysis

Cells were grown to 50-70% confluence in glass-bottom dishes (Nest, Wuxi, China), washed three times with PBST, and fixed in 4% PFA. For immunofluorescence staining, the cells were incubated with primary antibodies against E-cadherin, Snail, or PRL-3 (mice, Abcam, Cambridge, MA, USA) at 4°C overnight. After thorough washing, staining with Alexa-Fluor-488 conjugated goat anti-mouse and Alexa-Fluor-555 conjugated donkey anti-rabbit secondary antibodies was carried out at room temperature for 60 min, followed by DAPI nuclear counterstaining for 10 min. Finally, the cells were washed three times with PBST and photographed under a laser confocal microscope (Zeiss LSM710, Oberkochen, Germany). The data were processed with Adobe Photoshop 7.0 software (Newton, MA, USA).

RNA isolation and real-time quantitative polymerase chain reaction (PCR)

Total RNA was extracted using TRIzol reagent (Bio-Rad Laboratories, Hercules, CA, USA), and cDNA was synthesized with Prime Script RT (Bio-Rad Laboratories, Hercules, CA, USA) from 500 ng of RNA according to the manufacturer's protocol. Quantitative real-time PCR for VEGF (GAPDH was used an internal control) was performed using a Light Cycler 480 (Roche, Basel, Switzerland) and SYBR assay (Takara, Dalian, China). Band intensities were analyzed quantitatively using ImageJ software (NIH, Bethesda, USA).

Human miRNA arrays

For the secreted miRNA analysis, total RNA isolation was performed with the miRNeasy kit (Qiagen, Valencia, CA, USA) according to the manufacturer's protocol. The concentration and purity of the isolated RNA were determined using a spectrophotometer, and the integrity of the RNA was verified using an Agilent Eukaryote Total RNA Nano Series II chip on an Agilent 2100 BioAnalyzer. miRNA expression profiling of the samples was performed using the Affymetrix GeneChip miRNA 4.0 array platform (Affymetrix, Santa Clara, CA, USA) at the Johns Hopkins Deep Sequencing and Microarray Core (http://www.microarray.jhmi.edu/) according to the manufacturer's protocol. This array version covers all mature miRNA sequences.

Animals

Athymic nude mice were purchased from the Guangdong Provincial Medical Laboratory Animal Center, animal experiments were followed the NIH guidelines (NIH Pub. No. 85–23, revised 1996), and were approved by Animal Ethical and Welfare Committee of Sun Yat-sen University, and were performed according to the arrived guidelines 2.0. Mice were sacrificed by cervical dislocation in anaesthetized condition.

Xenograft mouse model

Athymic nude mice (BALB/c nu/nu, 6-week-old females) were used for liver metastasis assays via intrasplenic injection. A total of 200 μL of LoVo-P (PRL-3 stably transfected into LoVo cells) or LoVo-C (Control vector stably transfected into LoVo cells) cells at a concentration of 1×10^7 cells/mL was injected into the spleens of nude mice (n = 6 per group). The mice were housed in pathogen-free environments; they were checked, and data were recorded every 3 days. All animals were sacrificed on day 36, which were euthanized by an intraperitoneal injection of excessive pentobarbital. Livers and spleens were resected and photographed. For immunohistochemical staining, the livers were fixed in 4% paraformaldehyde and stained as described above.

Statistical analysis

Statistical analyses were performed using 18.0 SPSS software (SPSS, Chicago, IL, USA). All data are presented as the mean ± SD. Student's t-test was used to compare two independent groups of data. One-way analysis of variance (ANOVA) was used to analyze the significance among groups. Statistical tests for data analysis also included Fisher's exact and chi-square tests. Bivariate correlations between study variables were calculated by Spearman's rank correlation coefficients. P values < 0.05 were considered statistically significant.

Results

Correlation between E-cadherin and PRL-3 in primary site of CRC and liver metastases

To examine the relationship between the E-cadherin and PRL-3 expression in colorectal tumor and liver metastasis specimens, we performed IHC analyses of 75 human colorectal tumors. The tissue staining was calculated by the percentage of stained cells and the staining intensity. In the primary tumor samples, the level of E-cadherin expression was negatively associated with PRL-3 expression. However, in the colorectal liver metastasis tissues, a statistical analysis indicated an inverse correlation between the levels of E-cadherin and PRL-3 expression. However, the re-expression of E-cadherin was detected once CRC cells were colonized to the liver (Figure 1A-C). These results suggest that CRC cells undergo a change from EMT to MET in the progression of liver metastases.

Co-culture with hepatocytes results in the re-expression of E-cadherin in CRC cells

LoVo cells were used due to their low expression of endogenous PRL-3, and these cells were transfected with the PAcGFP-PRL-3/Control vectors (LoVo-P and LoVo-C). The expression of ectopic PRL-3 was verified by both western blot and real-time quantitative RT-PCR assays (Figure 2A). The expression of E-cadherin was lower in LoVo-P cells as we have previously demonstrated.[27] E-cadherin expression is a typical epithelial cell marker. To determine the role of hepatocytes in the progression of E-cadherin re-expression, we co-cultured LoVo-P cells with LO2 cells. Western blot analyses demonstrated that after co-culture with hepatocytes, the expression of E-cadherin was increased in a time-dependent manner. In contrast, the expression of snail, a prototypical mesenchymal marker, was significantly decreased in a time-dependent manner (Figure 2B). Immunofluorescence analyses were also carried out to further confirm the re-expression of E-cadherin and the down-regulation of snail (Figure 2C, D). Since Src plays an important role in regulating EMT through EGFR activation,[28] we next examined Src expression and EGFR activation in LoVo-P cells co-cultured with/without LO2 cells. The results showed that Src and EGFR activation were inhibited when LoVo-P cells were co-cultured with LO2 cells (Figure 2E). As invasion is an important consequence of MET, we investigated the impact of LoVo-P cells co-cultured with hepatocytes on invasion with transwell invasion assays. The result indicated that the invasion rates of LoVo-P cells co-cultured with LO2 cells decreased by 64% compared with those of LoVo-P cells cultured alone (Figure 2F). These results demonstrated that hepatocytes induced a change in co-cultured LoVo-P cells to the epithelial phenotype.

MiR-203a-3p of hepatocyte-derived exosomes cause the re-expression of E-cadherin through blocking Src expression

Exosomes play an important role in cell to cell communication and interaction. To determine whether hepatocyte-derived exosomes contribute to the change to MET, we first analyzed the structure of LO2-derived exosomes by electron microscopy; the results revealed a typical exosome structure and size of approximately 100 nm (Figure 3A, B). Exosome protein markers were examined by western blot (Figure 3C). To define the key factors of exosomes that inhibit Src expression, we used a human miRNA array and found that miR-203a-3p was increased and could potentially block Src expression (Figure 3D, E). Then, we transfected an exogenous miR-203a-3p mimic into LoVo-P cells; we found that Src expression and EGFR activation were inhibited, and the expression of E-cadherin was increased (Figure 3F, G). To provide direct evidence of the interaction between miR-203a-3p and Src, we used a luciferase reporter plasmid containing either the wild-type or mutant 3'-UTR of Src mRNA; the results showed that luciferase activity was reduced markedly in the cells transfected with the exogenous miR-203a-3p mimic, and the inhibitory activity of miR-203a-3p was lost when the binding sites were lost (Figure 3H). Moreover, invasion was also decreased when the exogenous miR-203a-3p mimic was transfected into LoVo-P cells (Figure 3I). These results demonstrate that miR-203a-3p increases E-cadherin levels and promotes LoVo-P cell MET through inhibiting Src expression.

MiR-203a-3p inhibited the Src/PKC/GSK-3β-mediated re-expression of E-cadherin

To explore the molecular mechanisms responsible for miR-203a-3p-induced MET in CRC cells, we detected the expression of Snail, which has been proven to repress the expression of E-cadherin.[28] The results indicated that the expression of Snail was gradually decreased when LoVo-P cells were transfected with the exogenous miR-203a-3p mimic, and the expression of E-cadherin was increased (Figure 4A). Because GSK-3β induces the phosphorylation of snail to cause its degradation and because GSK-3β phosphorylation induces GSK-3β inhibition, we further detected the expression of phosphorylated GSK-3β. The results showed that the expression of phosphorylated GSK-3β was decreased; this regulation was governed by PKC activity, which is a downstream molecule of the EGFR signaling pathway. Consistently, PKC phosphorylation was decreased in LoVo-P cells transfected with the exogenous miR-203a-3p mimic (Figure 4A).

To further confirm whether PKC activity was responsible for the Snail and E-cadherin regulation leading to MET, the PKC kinase inhibitor GF109203X was used. While PKC activation via phosphorylation was significantly reduced by PKC inhibitor treatment at the indicated time point, the results showed that Snail protein levels, as well as inhibitory GSK-3β phosphorylation, were significantly reduced, and E-cadherin expression was markedly increased (Figure 4B). Furthermore, reduced cell migration and invasion were observed following GF109203X treatment in a dose-dependent manner (Figure 4C). These data indicate that the increased E-cadherin expression in LoVo-P cells transfected with the exogenous miR-203a-3p mimic is due to Snail protein degradation, which is mediated by decreased PKC activity and subsequently increased GSK-3β activity.

Expression of miR-203a-3p and E-cadherin in vivo

In vivo animal model experiments were performed to examine the effects of PRL-3 on tumor metastasis. LoVo-P cells were administered to athymic nude mice via intrasplenic injection. More liver metastasis nodules were observed in the LoVo-P cell-injected group than in the LoVo-C cell-injected groups (Figure 5A-C). In addition, E-cadherin and miR-203a-3p expression was detected in the metastasis sites (Figure 5D, E). Moreover, the results showed that the expression levels of p-EGFR and p-PKC were decreased in the metastasis sites (Figure 5E). In 30 human CRC liver metastases samples, we performed IHC and qPCR analyses of miR-203a-3p, E-cadherin and Snail expression. The results showed that miR-203a-3p expression was similar to E-cadherin expression, but Snail was rarely expressed, which revealed the relationship between miR-203a-3p and E-cadherin/Snail (Figure 5F-H). These results demonstrate the correlation between miR-203a-3p and E-cadherin/Snail in liver metastases.

Discussion

Metastasis is the primary cause of death in patients with cancer, which is a multistep process including the detachment of cancer cells from the primary site and their transport into the blood vessels and colonization to distal organs; this process allows tumor cells to disseminate from their primary site and establish secondary tumors at secondary sites. Research has demonstrated that EMT is the main mechanism of this process.[29] Once tumor cells colonize distal organs, mesenchymal-to-epithelial transition (MET) may occur. However, the mechanism of successive EMT and MET switches remains unclear, and proposed mechanisms remain under discussion.[30] In this study, our research found that hepatocytes induced E-cadherin re-expression in PRL-3-overexpressing CRC cells, and this re-expression of E-cadherin is considered a marker of MET. Furthermore, miR-203a-3p from the exosomes of hepatocytes was found to inhibit Src expression and EGFR activation in CRC cells and to promote E-cadherin re-expression. In summary, our research determined that hepatocyte-derived miR-203a-3p induced MET in PRL-3-overexpressing CRC cells.

PRL-3 belongs to the protein-tyrosine phosphatase family, which plays a unique role in signal transduction. Researchers have noted that PRL-3 expression is higher in CRC metastases than in primary colorectal tumors and normal colon tissues, indicating that PRL-3 promotes the liver metastasis of CRC.[30] Numerous studies have revealed that the PI3K/AKT signaling pathway, integrin signaling pathway and Rho signaling pathway are the molecular mechanisms underlying cancer metastasis induced by PRL-3.[31] Furthermore, PRL-3 could recruit endothelial cells to promote angiogenesis.[32] Our previous research demonstrated that PRL-3 promotes CRC cell EMT, which is a major step in CRC cell liver metastasis. However, less is understood about how metastases are formed.

Exosomes are important for intracellular communication. Increased knowledge of the function of exosomes in cancer progression implies that the exosomal process is an orchestrated process. For example, research using the chorioallantoic membrane of chick embryos demonstrated that tumor cell

xenografts within the membrane required exosome release for directional movement.[33] Exosomes have a vast array of contents, which are composed of microRNAs, mRNA transcription factors and proteins and are highly variable and depend on cell origin.[34] MicroRNAs are small, non-coding RNAs that upon entering the recipient cell, bind to the target mRNA sequence and inhibit translation. Research has found that miRNAs can be used as diagnostic and prognostic biomarkers.[35] The shuttling of miRNA molecules that are either tumor-supportive or tumor-suppressive is important in cancer. In our research, we found that miR-203a-3p secreted by hepatocyte-derived exosomes specifically binds Src and inhibits Src expression and EGFR activation. The Src family of kinases comprises nine structural non-receptor tyrosine kinases. The activity of Src is increased in most solid tumors and some hematologic malignancies and is positively correlated with progressive stages of cancer.[36] Research has found that the tyrosine phosphorylation of β catenin and Tiam 1 by Src suppresses the association of β catenin with E-cadherin and disrupts the integrity of cell-to-cell junctions.[37] In addition, Src expression and activation in cancer cells always occurs after alterations to one or more of its activators, such as EGFR.[38] Interestingly, a study also revealed that PRL-3 could induce EGFR hyperactivation.[15] EGFR is a transmembrane receptor tyrosine kinase that is overexpressed in 49%-82% of CRC. EGFR overexpression could induce tumor cell EMT and then promote the progression and metastases of colorectal carcinoma.[39] To date, study has suggested that the inhibition of autocrine EGFR signaling increases E-cadherin expression and promotes EMT in human prostate carcinoma upon co-culture with hepatocytes.[40] In our research, Src was inhibited by miR-203a-3p, and EGFR activation and E-cadherin expression were inhibited; these findings are consistent with former results and indicate that hepatocytes promote high levels of PRL-3 expression in CRC cell MET through miR-203a-3p binding to Src and inhibiting EGFR activation.

To further detect the mechanism for MET in co-cultured CRC, we also detected Snail expression. Snail is a zinc-finger transcription factor that has been proven to directly bind to the E-boxes of the E-cadherin promoter and repress its expression. The data show that LoVo cell Snail expression levels were decreased, indicating that the accumulation of Snail was responsible for the repression of E-cadherin. It is well known that Snail is a substrate of GSK-3β. GSK-3β could phosphorylate Snail and promote its degradation through the ubiquitin-proteasome pathway. Previous research has also proven that PKC kinase could phosphorylate GSK-3β. In this study, we found that PRL-3 could induce the activity of PKC. When the PKC inhibitor GF 109203X was used, the phosphorylation of GSK-3β induced by PKC was completely inhibited, leading to the degradation of Snail. The data indicated that the down-regulation of the PKC/GSK-3β/Snail pathway was responsible for MET in CRC cells co-cultured with hepatocytes.

In summary, our study indicates that miR-203a-3p derived from hepatocyte exosomes plays an important role in promoting MET by inhibiting Src expression. The down-regulation of Src resulted in the inhibition of EGFR activation and the downstream signaling pathways and thus reduced the expression of E-cadherin, these results reveal the mechanism of liver metastases formation by CRC cells, which provides comprehensive insight into CRC liver metastasis.

Abbreviations

CRC: Colorectal Cancer cells

ZEB1: Zinc finger E-box Binding homeobox 1

ZEB2：Zinc finger E-box Binding homeobox 2

DMEM：Dulbecoo's Modified Eagle Medium

PBS: Phosphate Buffer Saline

PKC: Protein Kinase C

VEGF: Vascular Endothelial Growth Factor

EGFR：Epidermal Growth Factor Receptor

RIPA: Radio Immunoprecipitation Assay

PMSF: Phenylmethanesulfonyl Fluoride

GSK-3β: Glycogen synthase kinase-3β

Declarations

Availability of data and materials

The data used and/or analyzed during the current study are available from the corresponding author on reasonable request.

Acknowledgements

We thank colleagues from Key Laboratory of Malignant Tumor Molecular Mechanism and Translational Medicine of Guangzhou Bureau of Science and Information Technology for supporting this study.

Funding

This study was funded by National Natural Science Foundation of China (No. 81871981, 81702902, 8170111484) Natural Science Foundation of Guangdong Province (No. 2019A1515010646).

Authors' contributions

CZH and LW designed the project, LQS and XHY wrote the manuscript, YL and ZY finished the figure1 and 2, ZYJ finished figure 3, SPW finished figure 4, CZQ finished figure 5, all authors reviewed the manuscript.

Ethics Declarations

Ethics approval and consent to participate

Animal experiments were followed the NIH guidelines (NIH Pub. No. 85–23, revised 1996) and approved by the Animal Ethical and Welfare Committee of Sun Yat-sen University. The cell lines used in this study did not require ethics approval.

Consent for publication

Not applicable.

Conflicts of interest Statement

The authors declared that they have no conflicts of interest.

Competing interests

The authors declare that they have no competing interests.

Human Ethics

Patients are not involved in this study.

References

1. Hashimoto M, Kobayashi T, Tashiro H, Arihiro K, Kikuchi A, Ohdan H, h-Prune is associated with poor prognosis and epithelial-mesenchymal transition in patients with colorectal liver metastases. Int J Cancer, 2016, 139: 812-23
2. Siegel R, Naishadham D, Jemal A, Cancer statistics. CA Cancer J Clin, 2012, 62: 10-29
3. Chaffer CL, Weinberg RA, A perspective on cancer cell metastasis. Science , 2011, 331: 1559-64
4. Lamouille S, Xu J, Derynck R, Molecular mechanisms of epithelial-mesenchymal transition. Nat Rev Mol Cell Biol, 2014,15: 178-96

5. Zeisberg M, Shah AA, Kalluri R, Bone morphogenic protein-7 induces mesenchymal to epithelial transition in adult renal fibroblasts and facilitates regeneration of injured kidney. J Biol Chem, 2015, 280: 8094-100
6. Bae GY, Choi SJ, Lee JS, Jo J, Lee J, Kim J, et al, Loss of E-cadherin activates EGFR-MEK/ERK signaling, which promotes invasion via the ZEB1/MMP2 axis in non-small cell lung cancer. Oncotarget, 2013, 4: 2512-22
7. Alonso A, Sasin J, Bottini N, Friedberg I, Friedberg I, Osterman A, et al, Protein tyrosine phosphatases in the human genome. CELL, 2004,117: 699-711
8. Saha S, A Phosphatase Associated with Metastasis of Colorectal Cancer. Science 2001,294: 1343-1346
9. Wang H, Quah SY, Dong JM, Manser E, Tang JP, Zeng Q, PRL-3 Down-regulates PTEN Expression and Signals through PI3K to Promote Epithelial-Mesenchymal Transition. Cancer Res, 2007, 67: 2922-2926
10. Liu Y, Zhou J, Chen J, Gao W, Le Y, Ding Y, et al, PRL-3 promotes epithelial mesenchymal transition by regulating cadherin directly. Cancer Biol Ther, 2009,8: 1352-9
11. Hu L, Luo H, Wang W, Li H, He T, Poor prognosis of phosphatase of regenerating liver 3 expression in gastric cancer: a meta-analysis. Plos One, 2013, 8: e76927
12. Liu H, Al-aidaroos AQ, Wang H, Guo K, Li J, Zhang HF, et al, PRL-3 suppresses c-Fos and integrin alpha2 expression in ovarian cancer cells. BMC Cancer, 2013, 13: 80
13. Zhang J, Xiao Z, Lai D, Sun J, He C, Chu Z, Ye H, et al, miR-21, miR-17 and miR-19a induced by phosphatase of regenerating liver-3 promote the proliferation and metastasis of colon cancer. Br J Cancer, 2012, 107: 352-9
14. Lai W, Liu L, Zeng Y, Wu H, Xu H, Chen S, et al, KCNN4 channels participate in the EMT induced by PRL-3 in colorectal cancer. Med Oncol,2013, 30: 566
15. Al-Aidaroos AQ, Yuen HF, Guo K, Zhang SD, Chung TH, Chng WJ, et al, Metastasis-associated PRL-3 induces EGFR activation and addiction in cancer cells. J Clin Invest, 2013, 123: 3459-71
16. Epstein DM, Buck E, Old dog, new tricks: extracellular domain arginine methylation regulates EGFR function. J Clin Invest, 2014, 125**:** 4320-2
17. De Luca A, Maiello MR, D'Alessio A, Pergameno M, Normanno N, The RAS/RAF/MEK/ERK and the PI3K/AKT signalling pathways: role in cancer pathogenesis and implications for therapeutic approaches. Expert Opin Ther Targets, 2012, 16 Suppl 2**:** S17-27
18. Normanno N, Rachiglio AM, Lambiase M, Martinelli E, Fenizia F, Esposito C, et al, Heterogeneity of KRAS, NRAS, BRAF and PIK3CA mutations in metastatic colorectal cancer and potential effects on therapy in the CAPRI GOIM trial. Ann Oncol 2015, 26: 1710-4
19. Huang S, Holzel M, Knijnenburg T, Schlicker A, Roepman P, McDermott U, et al, MED12 controls the response to multiple cancer drugs through regulation of TGF-beta receptor signaling. Cell, 2012, 151: 937-50

20. Yates CC, Shepard CR, Stolz DB, Wells A, Co-culturing human prostate carcinoma cells with hepatocytes leads to increased expression of E-cadherin. Br J Cancer, 2011, 96: 1246-52
21. V. Harding, J.E. Heuser, P.D. Stahl, Exosomes: Looking back three decades and into the future, 2013, J Cell Biol, 200,367-371.
22. A. Melo, H. Sugimoto, J.T. O'Connell, N. Kato, A. Villanueva, A. Vidal, et al, Cancer exosomes perform cell-independent microRNA biogenesis and promote tumorigenesis, Cancer Cell, 2014, 26,707-721.
23. Vivian Yvonne Shin, Kent-Man Chu, MiRNA as potential biomarkers and therapeutic targets for gastric cancer, World J Gastroenterol. 2014 Aug 14; 20(30): 10432–10439.
24. He L, Hannon GJ, MicroRNAs: small RNAs with a big role in gene regulation.Nat Rev Genet. 2004 Jul; 5(7):522-31.
25. Yang Y, Li X, Du J, Yin Y, Li Y. Involvement of microRNAs-MMPs-E-cadherin in the migration and invasion of gastric cancer cells infected with Helicobacter pylori. Exp Cell Res. 2018 Jun 15;367(2):196-204.
26. Bradford, Marion, A Rapid and Sensitive Method for the Quantification of Microgram Quantities of Protein Utilizing the Principle of Protein-Dye Binding, Analytical Biochemistry. 1976, 72: 248–254.
27. Lai W, Chen S, Wu H, Guan Y, Liu L, Zeng Y, et al, PRL-3 promotes the proliferation of LoVo cells via the upregulation of KCNN4 channels. Oncol Rep 2011, 26: 909-17
28. Vu T, Datta PK, Regulation of EMT in Colorectal Cancer: A Culprit in Metastasis, Cancers (Basel). 2017, Dec 16;9(12).
29. Maejima Y, Ueba H, Kuroki M, Yasu T, Hashimoto S, Nabata A, et al, Src family kinases and nitric oxide production are required for hepatocyte growth factor-stimulated endothelial cell growth. Atherosclerosis. 2003 Mar; 167(1):89-95.
30. Thiery JP, Epithelial-mesenchymal transitions in tumour progression. 2002, Nat Rev Cancer 2: 442-54.
31. Kiesslich T, Pichler M, Neureiter D, Epigenetic control of epithelial-mesenchymal-transition in human cancer. Mol Clin Oncol 2013, 1: 3-11
32. Peng L, Jin G, Wang L, Guo J, Meng L, Shou C, Identification of integrin alpha1 as an interacting protein of protein tyrosine phosphatase PRL-3. Biochem Biophys Res Commun, 2006, 342: 179-83
33. Forte E, Orsatti L, Talamo F, Barbato G, De Francesco R, Tomei L, Ezrin is a specific and direct target of protein tyrosine phosphatase PRL-3. Biochim Biophys Acta 2008, 1783: 334-44.
34. H. Sung, T. Ketova, D. Hoshino, A. Zijlstra, A.M. Weaver, Directional cell movement through tissues is controlled by exosome secretion, Nat Commun, 2005, 6 ,7164.
35. Kawikova, P.W. Askenase, Diagnostic and therapeutic potentials of exosomes in CNS diseases, Brain Res, (2014), DOI: 10.1016/j.brainres.2014.09.070.
36. Falcone, A. Felsani, I. D'Agnano, Signaling by exosomal microRNAs in cancer, J Exp Clin Cancer Res, 2015, 34, 32.
37. Thomas SM, Brugge JS, Cellular functions regulated by Src family kinases. Annu Rev Cell Dev Biol. 1997; 13:513-609.

38. Rivard N, Phosphatidylinositol 3-kinase: a key regulator in adherens junction formation and function. Front Biosci (Landmark Ed). 2009 Jan 1;14:510-22.
39. Bromann PA, Korkaya H, Courtneidge SA, The interplay between Src family kinases and receptor tyrosine kinases. ONCOGENE, 2004, 23: 7957-68.
40. Spano JP, Lagorce C, Atlan D, Milano G, Domont J, Benamouzig R, et al, Impact of EGFR expression on colorectal cancer patient prognosis and survival. ANN ONCOL 2005, 16: 102-8.
41. Chao Y, Wu Q, Shepard C, Wells A. Hepatocyte induced re-expression of E-cadherin in breast and prostate cancer cells increases chemoresistance. Clin Exp Metastasis. 2012 Jan;29(1):39-50.

Figures

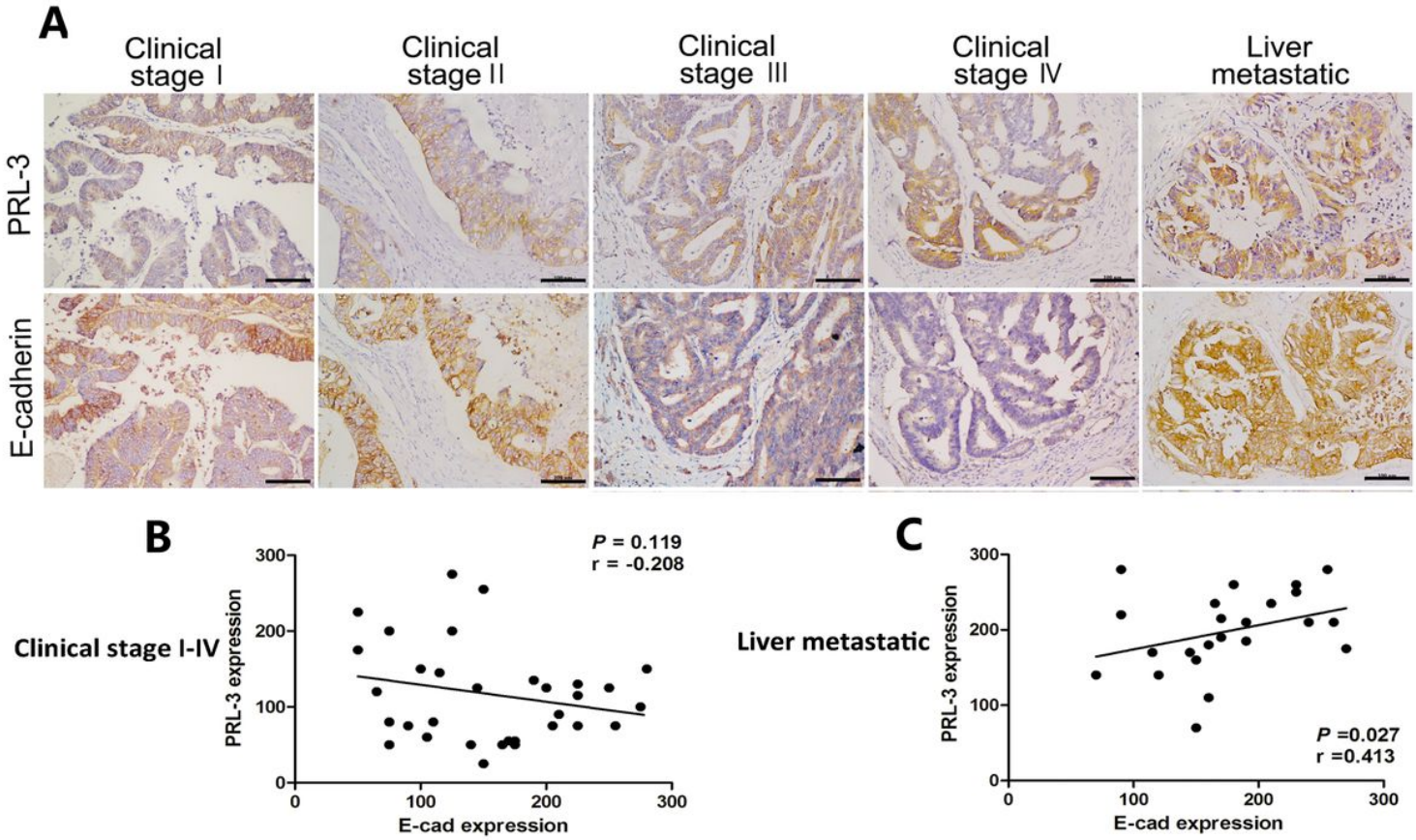

Figure 1

Clinically relevant expression of PRL-3 and E-cadherin in CRC tissues and liver metastases. Percentages of specimens showing low or high PRL-3 expression relative to the level of E-cadherin (E-cad) in CRC tissues (clinical stages I–IV) and in liver metastasis tissues (A). IHC staining shows the immunoreactivity of PRL-3 and E-cad in human CRC (clinical stages I–IV) and liver metastasis tissues. Original magnification, 200×. General correlation between relative PRL-3 and E-cad expression levels in CRC tissues (clinical stages I–IV) and in liver metastases in 23 samples (B-C).

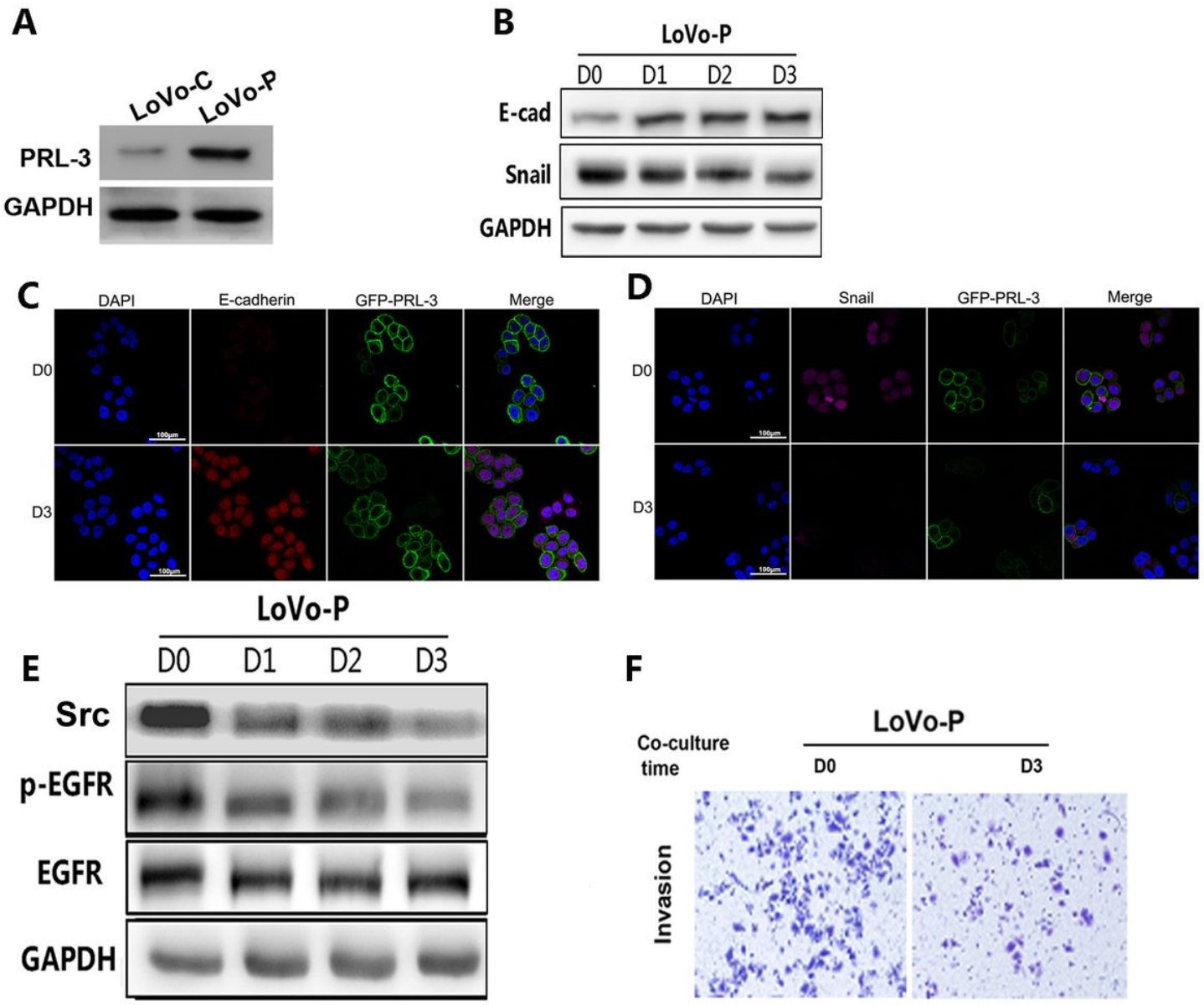

Figure 2

Co-culture with hepatocytes resulted in the re-expression of E-cadherin in CRC cells. (A) PRL-3 expression in stably transfected cell lines (LoVo-P and LoVo-C) was analyzed by western blotting. GAPDH served as the loading control. (B) LoVo-P cells were co-cultured with human hepatic LO2 cells for 0-3 days. The protein expression of E-cad and Snail were analyzed by western blotting. GAPDH served as the loading control. **P < 0.01. The immunoreactivity of E-cad (C) and Snail (D) detected by immunofluorescence staining. The nuclei were visualized with DAPI staining (blue). E-cadherin and Snail were immunostained with red, and PRL-3 was immunostained with green, and merged with blue. Original magnification, 400×. (E) Src and p-EGFR protein expression in LoVo-P cells co-cultured with LO2 cells was evaluated by western blot. (F) Images of invaded cells. Cells were co-cultured with human hepatic LO2 cells for 0/3

days and then harvested to perform invasion assays. The data represent the average of three independent experiments. **P < 0.01.

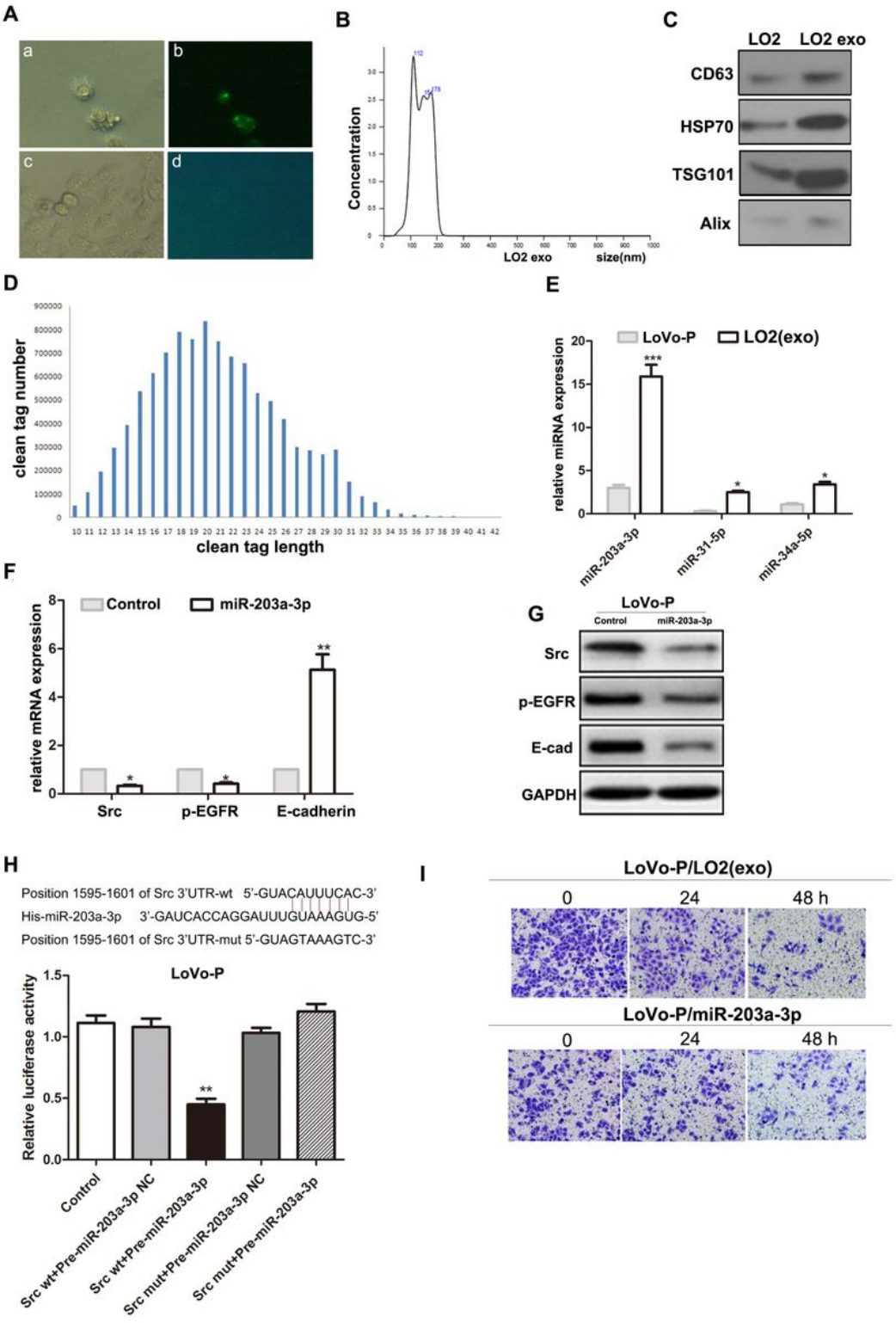

Figure 3

MiR-203a-3p of hepatocyte-derived exosomes caused the re-expression of E-cadherin through blocking Src expression. (A) Exosomes derived from LO2 cells were observed by electron microscopy: a. green labelled exosome from LO2 co-cultured with LoVo-P. b. Green labelled exosome co-cultured with LoVo-P

under fluorescence microscope. c. Unlabelled exosome from LO2 co-cultured with LoVo-P. d. Unlabelled exosome from LO2 co-cultured with LoVo-P under fluorescence microscope. (B) Wavelengths of exosomes. (C) CD63, HSP70 and TSG101 which are marker proteins in exosomes were examined by western blot. (D-E) A human miRNA array was used to screen miRNA expression in LO2-derived exosomes, the front 1000 kurtosis expression of microRNA (D), and the filtered microRNA results were confirmed by qPCR (E). (F-G) An exogenous miR-203a-3p mimic was transfected into LoVo-P cells, qPCR (F) and western blot (G) assays were used to examine the expression of Src, p-EGFR and E-cadherin. (H) Predicted binding sites of miR-203a-3p within the 3'-UTR of Src mRNA. (I) Transwell assays for number of invaded LoVo-P cells co-cultured with LO2 cells or transfected with the exogenous miR-203a-3p mimic. The data represent the average of three independent experiments. **P<0.01 compared with control.

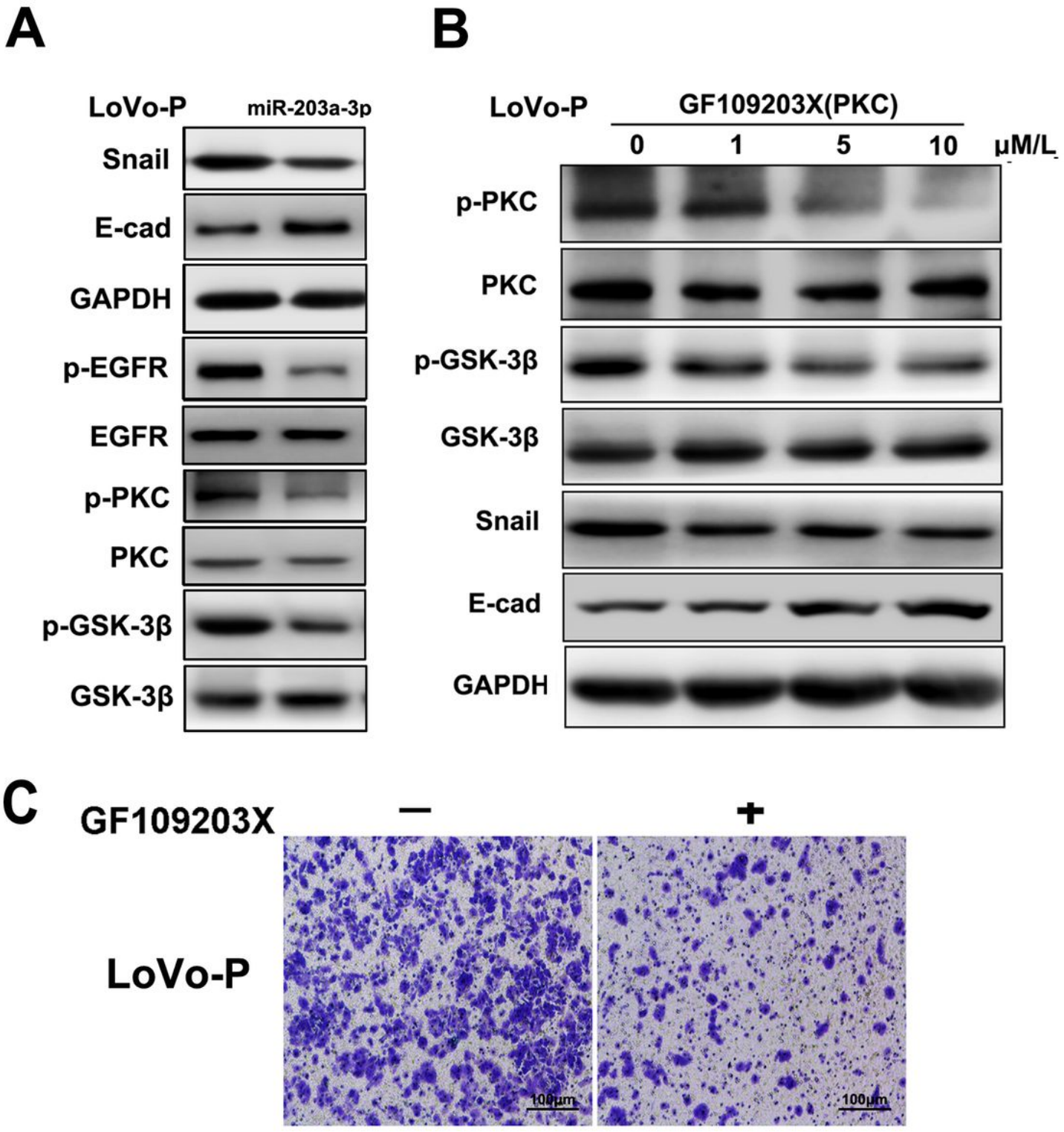

Figure 4

MiR-203a-3p inhibited the Src/PKC/GSK-3β-mediated re-expression of E-cadherin. (A) Expression of E-cadherin, Snail, p-EGFR, p-PKC and p-GSK-3β in LoVo-P cells transfected with the exogenous miR-203a-3p mimic. (B) Expression of E-cadherin, Snail, p-EGFR, p-PKC and p-GSK-3β in LoVo-P cells pretreated with various doses of GF109203X. (C) Invaded LoVo-P cells after pretreatment with PKC inhibitor GF109203X

and labelled with purple crystal. The data represent the average of three independent experiments. **P < 0.01.

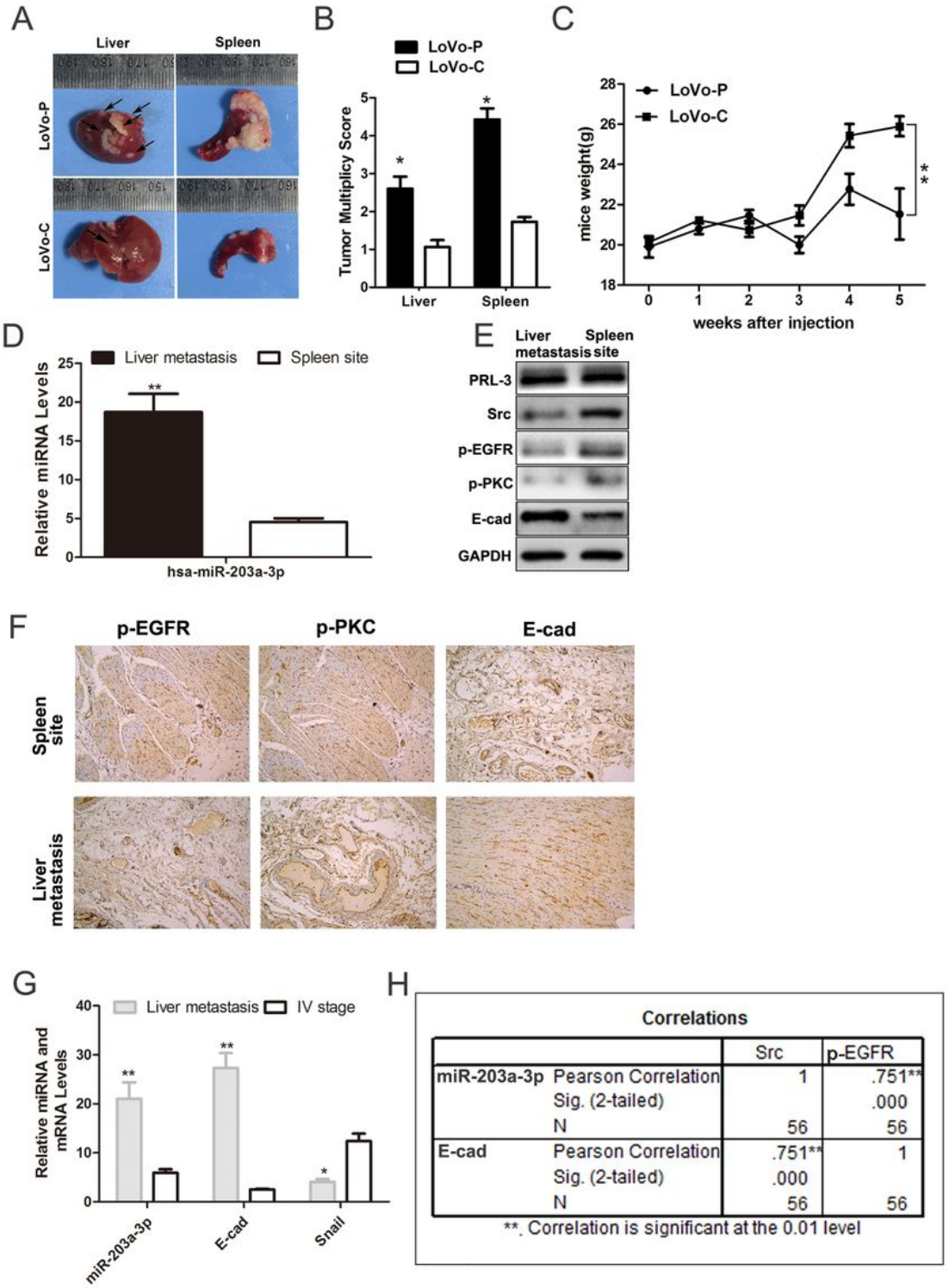

Figure 5

Expression of miR-203a-3p and E-cadherin in vivo. BALB/c-nu/nu female mice, 6- to 8-weeks-of-age, were divided randomly into 2 groups, separately injected LoVo-P / LoVo-C in spleens. (A) Image of tumor in spleen and liver. (B-C) Liver metastasis score and weight of mice. qPCR (D) and western blot assays (E)

examining the expression of miR-203a-3p, Src, p-EGFR, p-PKC and E-cadherin in the spleen site and liver metastases. (F) IHC examining the p-EGFR, p-PKC and E-cadherin immunoreactivity in the spleen site and liver metastases. (G) Expression of miR-203a-3p/E-cadherin (E-cad)/Snail in the primary site and liver metastases. (H) Correlation between miR-203a-3p/E-cadherin (E-cad) and Src/p-EGFR expression.